

# Identification of Hydrophobic Amino Acid Residues Involved in the Formation of S100P Homodimers in Vivo<sup>†</sup>

Max Koltzsch and Volker Gerke\*

*Institute for Medical Biochemistry, University of Münster, Von Esmarch Strasse 56, 48129 Münster, Germany*

*Received February 3, 2000; Revised Manuscript Received May 5, 2000*

**ABSTRACT:** S100 proteins are small dimeric members of the EF-hand superfamily of Ca<sup>2+</sup> binding proteins thought to participate in mediating intracellular Ca<sup>2+</sup> signals by binding to and thereby regulating target proteins in a Ca<sup>2+</sup>-dependent manner. As dimer formation is crucial to S100 function, we applied a yeast two-hybrid approach in analyzing in vivo molecular aspects of S100 dimerization. We chose S100P, a member of the S100 family highly expressed in placenta, for detailed analysis and showed that S100P monomers strongly interact with one another but not with other S100 polypeptides, indicating that homodimer formation is obligatory for S100P. Analysis of the interaction of site-specific S100P mutants with the wild-type polypeptide or with other S100P mutant chains identifies conserved hydrophobic amino acid residues involved in mediating dimerization in vivo. Of these residues, F-15 is crucially important as a mutation to alanine abolishes dimerization even when the F15A S100P mutant polypeptide is allowed to interact with a wild-type chain. On the other hand, I-11, I-12, or F-89 need to be replaced by a less hydrophobic residue in both subunits for there to be a similar extent of interfere with dimerization. This proves that hydrophobic residues implicated through structural studies in S100 dimerization are involved in the dimer interaction in vivo and argues for a hierarchy of hydrophobic contacts stabilizing the dimer and thereby regulating S100 function.

Intracellular Ca<sup>2+</sup> binding proteins (CaBPs) participate in transducing Ca<sup>2+</sup> signals, i.e., transient rises in intracellular Ca<sup>2+</sup> concentrations, into cellular responses. In contrast to proteins involved in Ca<sup>2+</sup> buffering and homeostasis, the conformation and activity of CaBPs participating in stimulus–response coupling are modulated by Ca<sup>2+</sup> binding (1). According to the architecture of their Ca<sup>2+</sup> binding sites, CaBPs are grouped into distinct families with the EF-hand superfamily containing the largest number of proteins. EF-hand denotes the Ca<sup>2+</sup> binding motif which consists of two  $\alpha$ -helices [the E- and F-helix in parvalbumin (2)] flanking an interhelical loop providing carbonyl and carboxyl ligands for Ca<sup>2+</sup> coordination (3). S100 proteins comprise a large subfamily within the EF-hand superfamily. They are characterized by a pair of EF-hands connected through a short linker sequence and by an often extended E- and F-helix of the first and second EF-hand, respectively. The two EF-hands of S100 proteins differ in their structure and affinity for Ca<sup>2+</sup> ions with the N-terminal, noncanonical EF-hand generally having a lower affinity than the canonical C-terminal EF-hand. With the exception of calbindin 9k, S100 proteins form homo- and in some cases heterodimers, and dimer formation has been considered obligatory for S100 function (4, 5). Like other EF-hand proteins such as calmodulin and myosin light chain, S100 proteins are thought to bind to and thereby regulate cellular target proteins in their Ca<sup>2+</sup>-bound conformation. S100 targets that have been identified so far include

cytoskeletal proteins such as intermediate filament proteins, microtubule-associated  $\tau$  proteins, and the actin capping protein CapZ, enzymes such as fructose aldolase, the myosin-associated giant twitchin kinase or guanylate cyclase, and members of the annexin family of Ca<sup>2+</sup>-regulated membrane proteins. However, in contrast to the ubiquitously expressed calmodulin, S100 proteins are often synthesized in a tissue-specific manner, and it is discussed that the whole family has evolved to fine-tune S100-mediated Ca<sup>2+</sup> signaling in different types of cells by optimizing S100–target protein interactions (1, 4–6).

While the structure of the only monomeric S100 protein calbindin 9k has been known for some time, structures of dimeric S100 proteins (S100B, S100A6, S100A10, and S100A11) have only been determined in recent years by NMR spectroscopy and X-ray crystallography approaches (7–15). Three important principles emerged through these analyses. First, the S100 dimers are stabilized through a number of hydrophobic interactions involving five aliphatic or aromatic side chains found at positions conserved within the family. Second, dimer formation via the same principle occurs in the presence and absence of Ca<sup>2+</sup>. Third, conformational changes elicited by Ca<sup>2+</sup> binding expose hydrophobic residues in helices I and IV, i.e., the E-helix of the first and the F-helix of the second EF-hand, which then are able to participate in target protein binding. In the few high-resolution structures of S100 proteins complexed to their target peptides, it is evident that residues from both subunits of the S100 dimer make contacts with the target peptide and that two target peptides are bound per S100 dimer in a highly symmetric fashion (11, 12).

<sup>†</sup> Financial support by the Deutsche Forschungsgemeinschaft is gratefully acknowledged.

\* Corresponding author. Telephone: 0049 251 8356722. Fax: 0049 251 8356748. E-mail: gerke@uni-muenster.de.

Table 1: Oligonucleotides Used To Generate WT S100P Chains and Mutant Derivatives by PCR<sup>a</sup>

S100P-WT 5'	5'-GATCGAATTC ATG ACG GAA CTA GAG ACA GCC ATG-3'
S100P-A7I 5'	5'-GATCGAATTC ATG ACG GAA CTA GAG ACA <b>ATC</b> ATG GGC ATG-3'
S100P-I11A 5'	5'-GATCGAATTC ATG ACG GAA CTA GAG ACA GCC ATG GGC ATG <b>GCT</b> ATA GAC GTC-3'
S100P-I12A 5'	5'-GATCGAATTC ATG ACG GAA CTA GAG ACA GCC ATG GGC ATG ATC <b>GCT</b> GAC GTC-3'
S100P-F15A 5'	5'-GATCGAATTC ATG ACG GAA CTA GAG ACA GCC ATG GGC ATG ATC ATA GAC GTC <b>GCT</b> TCC CG-3'
S100P-I12A/F15A 5'	5'-GATCGAATTC ATG ACG GAA CTA GAG ACA GCC ATG GGC ATG ATC <b>GCT</b> GAC GTC <b>GCT</b> TCC CG-3'
S100P-WT 3'	5'-GATCGTCGAC TCA TTT GAG TCC TGC CTT CTC AAA G-3'
S100P-F89A 3'	5'-GATCGTCGAC TCA TTT GAG TCC TGC CTT CTC <b>AGC</b> GTA CTT G-3'
S100P-C85A 3'	5'-GATCGTCGAC TCA TTT GAG TCC TGC CTT CTC AAA GTA CTT GTG <b>AGC</b> GGC AGA CG-3'
S100P-S83I 3'	5'-GATCGTCGAC TCA TTT GAG TCC TGC CTT CTC AAA GTA CTT GTG ACA GGC <b>AAT</b> CGT GAT TG-3'
S100P-S83I/F89A 3'	5'-GATCGTCGAC TCA TTT GAG TCC TGC CTT CTC <b>AGC</b> GTA CTT GTG ACA GGC <b>AAT</b> CGT GAT TG-3'

<sup>a</sup> Restriction enzyme recognition sequences are underlined, and the reading frame of S100P is depicted in triplets. The bold letters denote residues altered for S100P mutagenesis.

With the exception of the S100A8–S100A9 heterodimer (16), no information about S100 protein dimerization in living cells is available to date. To address this problem, we chose the yeast two-hybrid system (17) and analyzed the interaction of two S100P chains in vivo. S100P is a member of the family primarily expressed in placenta whose cellular target has remained elusive so far but whose biochemical and biophysical properties have been studied in detail (18, 19). By introducing single-site mutations and by analyzing the interaction of S100P mutant chains with one another and with the wild-type polypeptide, we identified hydrophobic residues in helices I and IV which participate to varying degrees in homodimer formation in vivo.

## EXPERIMENTAL PROCEDURES

**Construction of Plasmids.** The cDNA encoding WT human S100P was generated by polymerase chain reaction using a human placental MATCHMAKER cDNA library in pACT2 (Clontech) as a template. PCR<sup>1</sup> was carried out using high-fidelity *Pfu* DNA polymerase (Stratagene) and oligonucleotide primers containing appropriate restriction sites. Amino acid substitutions resulting in mutant S100P proteins were generated by using mutated primers for the PCR. All primers are summarized in Table 1.

cDNA products of the PCRs were cloned into the yeast plasmid pBD Gal4 cam or pAD Gal4 (Stratagene) in frame with either the DNA-binding domain or the transcription activating domain of Gal4, respectively. For each construct, the same restriction endonuclease sites were used. This ensured that all fusion proteins of S100P and Gal4 domains harbored the same additional amino acids encoded by the multiple-cloning site. The correctness of all constructs was verified by sequence analysis.

**Yeast Transformation and the Two-Hybrid Interaction Assay.** The *Saccharomyces cerevisiae* strain Y190 (*MATa*, *ura3-52*, *his3-200*, *ade2-101*, *lys2-801*, *trp1-901*, *leu2-3*, *112*, *gal4Δ*, *gal80Δ*, *cyh2*, *LYS2::GAL1<sub>UAS</sub>-HIS3<sub>TATA</sub>-HIS3*, *URA3::GAL1<sub>UAS</sub>-GAL1<sub>TATA</sub>-lacZ*) was cotransformed with different plasmids using the “high-efficiency lithium acetate/single-stranded carrier DNA/polyethylene glycol” method described by Gietz et al. (<http://www.umanitoba.ca/faculties/medicine/>

units/human\_genetics/gietz/method.html). Transformed cells were grown for 3 days at 30 °C on SD glucose agar plates to select for the presence of both plasmids. For selection of interacting sequences, cells were transferred to SD glucose agar plates containing 40 mM 3-AT and lacking the amino acids leucine, tryptophan, and histidine and incubated for an additional 4 days at 30 °C.

Colony lift filter assays were employed to analyze for  $\beta$ -galactosidase activity. Therefore, the colonies were transferred to nitrocellulose membranes (Schleicher & Schuell), frozen in liquid nitrogen for 10–20 s, placed on top of another filter (Schleicher & Schuell GB 002) presoaked in a Z-buffer/X-Gal/ $\beta$ -mercaptoethanol mixture [60 mM Na<sub>2</sub>HPO<sub>4</sub>, 40 mM NaH<sub>2</sub>PO<sub>4</sub>, 100 mM KCl, 1 mM MgSO<sub>4</sub> (pH 7.0), 0.27% (v/v)  $\beta$ -mercaptoethanol, and 0.334% (w/v) X-Gal], and finally incubated at 30 °C until blue colors developed (maximum of 16 h).

**Yeast Two-Hybrid Screening.** To screen for putative ligands of S100P, a human placental cDNA library in pACT2 (Clontech) was used. The plasmid pBD Gal4 cam (Stratagene), encoding the bait fusion protein (binding domain of Gal4/S100P WT), was cotransformed with the library plasmids into Y190 yeast cells, followed by incubation of the transformed cells on selective agar plates lacking amino acids leucine, tryptophan, and histidine (with 25 mM 3-AT) to select for interacting sequences. Plates were incubated for up to 10 days at 30 °C to allow for the detection of weak interactions. Subsequently, visible colonies were transferred to fresh selection plates, incubated for an additional 4 days, and then subjected to colony filter lift assays. PCRs employing lysed yeast cells (positive clones) were carried out to amplify the cDNA inserts of pACT2. Products of the reactions were subjected to restriction analyses, and the cDNA inserts were divided into groups according to their restriction patterns. pACT2-derived plasmids from each group were rescued from the yeast cells and used to cotransform yeast together with the empty pBD Gal4 cam to confirm the specificity of the observed interactions. The library cDNAs of remaining positive clones, i.e., those only growing when the S100P-containing bait vector was used in the cotransformation, were analyzed in detail by restriction analysis and sequencing.

**Quantification of Interaction.** The strength of interaction between different S100P chains, expressed as fusions with the binding or activation domain of Gal4, was determined by measuring the expression level of the lacZ reporter gene. Therefore, at least five independent yeast clones from each cotransformation were picked and cultured overnight in 5

<sup>1</sup> Abbreviations: 3-AT, 3-amino-1,2,4-triazole; EDTA, ethylenediaminetetraacetic acid; EGTA, ethylene dioxy-bis(ethylenenitrilo)-tetraacetic acid; IPTG, isopropyl  $\beta$ -D-thiogalactopyranoside; PCR, polymerase chain reaction; PMSF, phenylmethanesulfonyl fluoride; SDS–PAGE, sodium dodecyl sulfate–polyacrylamide gel electrophoresis; WT, wild-type; X-Gal, 5-bromo-4-chloro-3-indolyl  $\beta$ -D-galactoside.

mL of synthetic medium lacking leucine, tryptophan, and histidine. Subsequently, the cultures were inoculated into fresh rich medium (YPD) and incubated at 30 °C with agitation until they reached mid log phase ( $OD_{600} = 0.6-0.8$ ). Yeast cells were then harvested by centrifugation (1000g for 5 min), suspended in Z-buffer, and lysed by three freeze-thaw cycles. *O*-Nitrophenyl  $\beta$ -D-galactopyranoside (ONPG) was added to the lysate, and the mixture was incubated at 30 °C until a yellow color developed. The reaction was stopped by adding  $Na_2CO_3$  to a final concentration of 300 mM, and the absorbance was measured at 420 nm.  $\beta$ -Galactosidase activity was calculated from this value and expressed as Miller units. For a relative comparison, the  $\beta$ -galactosidase activity of each fusion protein pair was defined arbitrarily with the interaction between the S100P WT proteins set to 100%.

**Preparation of Yeast Protein Extracts for Western Blot Analysis.** Following overnight incubation of transformed yeast cells in 5 mL of selective medium, 50 mL of rich YPD medium was inoculated with the starter culture and cells were grown until the culture reached an  $OD_{600}$  of 0.4–0.6. The culture was then chilled quickly by adding an equal volume of ice, and cells were harvested by centrifugation. After a wash with ice-cold water, the cell pellet was frozen in liquid nitrogen and then resuspended in 100  $\mu$ L of prewarmed (60 °C) cracking buffer [40 mM Tris-HCl (pH 6.8), 8 M urea, 5% (w/v) SDS, 0.1 mM EDTA, 0.4 mg/mL bromphenol blue, 100 mM  $\beta$ -mercaptoethanol, 10  $\mu$ g/mL pepstatin A, 3  $\mu$ M leupeptin, 14 mM benzamidine, 35  $\mu$ g/mL aprotinin, and 1 mg/mL PMSF] per 7.5  $OD_{600}$  units of cells. Glass beads ( $\varnothing \sim 0.5$  mm) were added to the cells, and the suspension was heated at 70 °C for 10 min and then vortexed vigorously for at least 2 min. The suspension was centrifuged (14 000 rpm for 5 min) and the supernatant chilled on ice. The pellet that was obtained was heated to 100 °C for 3–5 min, vortexed again, and subjected to an additional centrifugation (14 000 rpm for 5 min). The resulting supernatant was combined with the first supernatant and the mixture subjected to SDS-PAGE (20).

**Western Blot Analysis.** To confirm that the fusion proteins were expressed in the transformed yeast cells, Western blot analyses were performed using a monoclonal antibody directed against the GAL4 DNA-binding domain (Clontech). Protein extracts from transformed yeast cells were separated in 12.5% tris/tricine/SDS gels (21) and transferred to PVDF membrane (Millipore Corp.). Membranes were blocked with 4% bovine serum albumin (BSA) in TBS and 0.02% Tween (TBS-T) and probed with primary antibodies followed by incubation with HRP-conjugated goat anti-mouse IgGs (Jackson Immuno Research; 1:10000 in TBS-T, 4% BSA) as secondary antibodies and detection by chemoluminescence (ECL, Pierce Chemical Co.).

**Recombinant Expression and Purification of S100P F15A.** cDNA encoding the F15A S100P mutant was cloned into the *Eco*RI–*Sal*I linearized pET 28a+ vector (Novagen). The resulting construct encoding F15A S100P with an N-terminal histidine tag was used to transform *Escherichia coli* cells [strain BL21(DE3)pLysS]. For protein expression, transformed bacteria were grown to an  $OD_{600}$  of 0.6 and recombinant protein expression was then induced by adding IPTG to a concentration of 1 mM. Following incubation for an additional 3 h, cells were harvested by centrifugation

(5000g for 10 min), resuspended in lysis buffer [50 mM Tris-HCl (pH 7.5), 300 mM NaCl, 20 mM imidazole-HCl (pH 7.5), 1 mM EDTA, 10 mM  $\beta$ -mercaptoethanol, 1 mM PMSF, and 10  $\mu$ M leupeptin], and lysed by repeated freeze-thaw cycles (three times) and sonication. The lysate was centrifuged for 1 h at 100000g, and the supernatant that was obtained was made 5 mM in  $Ca^{2+}$  and applied to a phenyl-Sepharose (Pharmacia) column equilibrated in lysis buffer containing 0.5 mM  $Ca^{2+}$  and no EDTA. Following extensive washing with the same buffer, bound protein was eluted with 30% 2-propanol in lysis buffer containing 1 mM EGTA. F15A S100P-containing fractions were pooled, dialyzed against 20 mM imidazole (pH 7.5), 300 mM NaCl, 10 mM  $\beta$ -mercaptoethanol, and 1 mM PMSF, and applied to a Ni-NTA agarose (Qiagen) column equilibrated in the same buffer. F15A S100P was eluted with 250 mM imidazole (pH 7.5), 300 mM NaCl, 10 mM  $\beta$ -mercaptoethanol, and 1 mM PMSF.

## RESULTS

**Homodimer Formation of S100P.** The yeast two-hybrid system was used to analyze in vivo the dimerization of S100P. In a first approach, we tested whether homodimer formation is obligatory or whether S100P can engage in heterodimeric complexes with other S100 proteins. Such heterocomplexes have been described, e.g., for S100A1, S100B, S100A8, and S100A9 (22, 23). WT S100P cDNA was cloned into Gal4 activation (pAD) or DNA-binding domain (pBD) vectors, and interaction with S100A10 or S100A11 was analyzed in yeast clones cotransformed with pAD-S100 or pBD-S100, respectively. In these and the following experiments, expression of the recombinant BD-fusion proteins in the transformed yeast cells was routinely analyzed by immunoblotting to verify that a lack of interaction signal is not due to a lack of recombinant fusion protein (not shown). With the exception of the pAD-S100P–pBD-S100P pair (and pAD-S100A11–pBD-S100A11 used as control), no combination of pAD-S100P or pBD-S100P with other activation or binding domain constructs resulted in growth on Leu-, Trp-, and His-negative agar plates (Figure 1). This suggested that S100P is not capable of forming heterodimers with other S100 proteins. To generalize this conclusion, we screened a placental cDNA library (Clontech) for interaction partners using S100P as bait. Four hundred positive clones were obtained in a total of  $1 \times 10^7$  that were screened. A detailed restriction and sequence analysis revealed that all positive clones encoded S100P, further strengthening that homodimer formation is obligatory for this S100 protein (not shown). This is in contrast to, for example, S100A1 which forms heterodimers with S100B and, as revealed in a more recent work with a two-hybrid approach, also interacts with S100A4 (24).

**Residues Participating in S100P Homodimer Formation.** To identify single amino acid side chains involved in S100P homodimer formation, we generated a series of mutant cDNAs by site-specific mutagenesis. The different cDNAs were cloned into the pAD or pBD expression vector, and their capability of interacting with one another or with other S100P mutants was analyzed following cotransformation into yeast Y190 cells. In addition to revealing the interaction in a living cell, this approach offers the advantage that individual mutant molecules can be screened against the wild



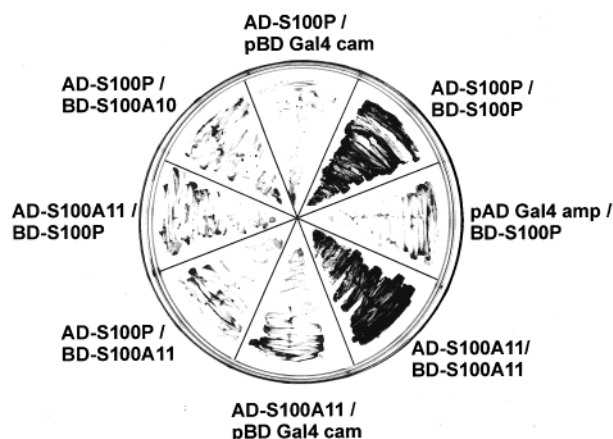


FIGURE 1: Specificity of S100P homodimer formation. Yeast Y190 cells were cotransformed with the indicated sets of plasmids and grown for 4 days at 30 °C on synthetic selection medium containing 40 mM 3-AT and lacking the amino acids leucine, tryptophan, and histidine. AD- and BD-S100 denote activation domain and binding domain vector with the respective S100 protein insert. Growth indicating interaction is only observed when both AD and BD plasmids contain the S100P or S100A11 insert but not when the Gal4 domains (pBD Gal4 cam and pAD Gal4 amp) or S100A10 and S100A11 fusion proteins are coexpressed with S100P fusions.

type or other mutant molecules; i.e., a single-site mutant fused to the AD can be used in cotransformation experiments with pBD vectors containing the same mutant cDNA, another mutant cDNA, or the WT S100P cDNA. Residues mutated individually or in pairs in the different S100P derivatives are given in Figure 2 which shows the S100P sequence in comparison to that of other human S100 proteins. Our

analyses focused on hydrophobic side chains (I-11, I-12, and F-15) which in a sequence alignment reside in positions identified in structural studies of other S100 proteins as potentially essential dimer contacts (7, 8, 10, 11, 13, 15, 25). In other S100 proteins, the dimer interface is formed by two clusters of hydrophobic residues and the sequence alignment indicates that I-11 lies in one and I-12 in the other such potential cluster in S100P. We also replaced F-89 with a less hydrophobic residue as a side chain at the corresponding position had been implicated in dimer contact in S100A6 (7) but appeared to be less important for dimerization in S100A10 and S100A11 (26, 27). Moreover, we subjected C-85 to a more detailed scrutiny as a cysteine at homologue positions was shown to be crucially important for target protein binding in S100A10 (26, 28). Finally, S-83 was mutated to a more hydrophobic residue (I) since a hydrophobic side chain is almost invariant at the homologue position in other proteins of the family where it has been implicated in mediating dimerization (7).

Following cotransformation, the resulting clones were assayed for growth on selective media and for  $\beta$ -galactosidase activity in a colony filter lift assay. The results are summarized in Figure 3 with both assays yielding to a large extent superimposable data. On the basis of these observations, the mutants can be subdivided into three groups. First, replacing the hydrophobic residue I-11, I-12, or F-89 or the cysteine at position 85 with alanine results in S100P derivatives that are still capable of interacting with the WT molecule. However, when the I11A, I12A, or F89A mutation is introduced in both two-hybrid fusion proteins, i.e., present

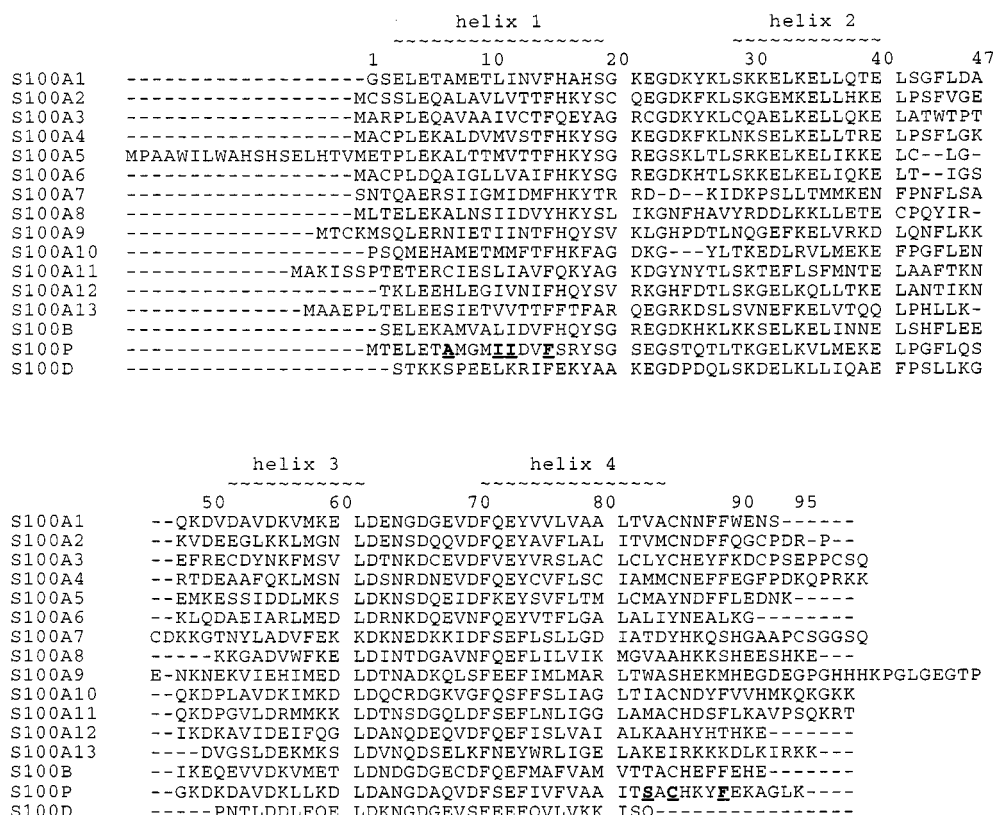


FIGURE 2: Best-fit alignment of human S100 proteins. Underlined bold letters indicate amino acid residues mutated in the S100P proteins employed in this study. Residues in positions 11, 12, 15, 85, and 89 were changed to alanine (A), and residues in positions 7 and 83 were replaced with isoleucine (I). Numbering is based on the sequence of the S100P protein. The ~ symbols indicate areas with  $\alpha$ -helical structures (helices 1 and 2 of the N-terminal EF-hand and 3 and 4 of the C-terminal EF-hand).

A											
AD-BD	AD	WT	I11A	I12A	I12A F15A	F15A	I12A F89A	F89A	S83I	S83I F89A	C85A
BD	-	-	-	-	-	-	-	-	-	-	-
WT	-	+++	++	++	-	-	-	++	++	++	+++
I11A	-	++	+	+	-	-	-	+	++	+	+
I12A	-	++	n.d.	++	-	-	-	+	+	+	+
I12A F15A	-	-	n.d.	-	-	-	-	-	-	-	-
F15A	-	-	n.d.	-	-	-	-	-	-	-	-
I12A F89A	-	-	n.d.	-	-	-	-	+	+	+	+
F89A	-	+++	n.d.	+++	-	-	-	+	+++	+++	++
S83I	-	+++	n.d.	+++	-	-	-	++	+++	+++	+++
S83I F89A	-	+++	n.d.	+++	-	-	+	+++	+++	++	+++
C85A	-	+++	n.d.	+++	-	-	+	+	+++	+++	++

B											
AD-BD	AD	WT	I11A	I12A	I12A F15A	F15A	I12A F89A	F89A	S83I	S83I F89A	C85A
BD	-	-	-	-	-	-	-	-	-	-	-
WT	-	+++	++	+++	-	-	-	+++	+++	+++	+++
I11A	-	++	+	-	-	-	-	+	++	+	+
I12A	-	+	n.d.	-	-	-	-	++	+	+	++
I12A F15A	-	-	n.d.	-	-	-	-	-	-	-	-
F15A	-	-	n.d.	-	-	-	-	-	-	-	-
I12A F89A	-	-	n.d.	-	-	-	-	-	-	-	-
F89A	-	++	n.d.	+++	-	-	-	-	++	+	+
S83I	-	+++	n.d.	++	-	-	-	+++	++	++	++
S83I F89A	-	+++	n.d.	++	-	-	-	++	++	+	++
C85A	-	++	n.d.	++	-	-	-	+	++	+	+

FIGURE 3: (A) Growth of cotransformed Y190 yeast cells on Leu-, Trp-, and His-negative agar plates containing 40 mM 3-AT. Yeast cells were cotransformed with the appropriate sets of plasmids indicated in the chart. The ability to grow was estimated after a 4 day incubation from the size of resulting colonies and taken as an indicator for the strength of interaction between the expressed AD and BD fusion proteins. AD and BD, activation domain vector pAD Gal4 amp and binding domain vector pBD Gal4 cam containing no insert, respectively. WT, AD or BD vector containing the WT S100P insert. I11A, I12A, F15A, F89A, etc., AD or BD vector with the respective mutant S100P insert. A minus sign (-) denotes no growth, whereas +, ++, and +++ indicate weak, medium, and very good growth, respectively. (B)  $\beta$ -Galactosidase activity of cotransformed yeast cells. Y190 cells were cotransformed with the indicated AD and BD fusion plasmids, and following incubation for 4 days, the resulting  $\beta$ -galactosidase activity was estimated according to the blue color of yeast replicas after colony filter lift assays. AD and BD, activation domain vector pAD Gal4 amp and binding domain vector pBD Gal4 cam containing no insert, respectively. WT, AD or BD vector containing the WT S100P insert. I11A, I12A, F15A, F89A, etc., AD or BD vector with the respective mutant S100P insert. A minus sign (-) denotes background activity, whereas +, ++, and +++ indicate the development of a light blue color, the development of a blue color, and the quick development of a dark blue color, respectively.

in the pAD-S100P and pBD-S100P vectors, the resulting cotransformants are impaired in their growth on selective media and their  $\beta$ -galactosidase activity. Thus, dimer formation is compromised to some extent only when both subunit chains carry the respective amino acid substitutions. F15A S100P and the double mutants I12A/F15A S100P and I12A/F89A S100P fall into a second category. Hardly any growth or  $\beta$ -galactosidase activity is observed when these mutant derivatives are coexpressed together with WT S100P or any of the other mutants employed in this study. Therefore, introducing a less hydrophobic side chain at position 15 or, simultaneously, at positions 12 and 89 critically interferes with dimerization even when these mutations are only present in one of the two subunits. S83I is a third type of mutation wherein introducing a more hydrophobic side chain generates a mutant protein exhibiting increased dimer stability when compared to that of WT S100P.

Of all the mutants that have been analyzed, F15A is the only one exhibiting no interaction with WT S100P. Since a residue at the corresponding position had been implicated in interhelical contact stabilizing, for example, the monomeric subunit of  $\text{Ca}^{2+}$ -bound S100B (15), we analyzed whether the F15A replacement would render the S100P monomer less stable due to a disruption of its hydrophobic core. Therefore, a His-tagged version of F15A S100P was expressed recombinantly in bacteria, and its properties were compared to those of His-tagged WT S100P. As observed for WT S100P (not shown), F15A S100P is expressed as a soluble protein and can be purified on phenyl-Sepharose and

Ni agarose (Figure 4). This indicates that monomer stability is not significantly affected by the F15A mutation and that the effects observed in our two-hybrid analyses reflect an impaired ability of the F15A mutant chain to dimerize.

To gain a more quantitative insight into the stability of the respective dimers that formed, we determined  $\beta$ -galactosidase activity in extracts of yeast cells cotransformed with pAD S100P-WT, -F89A, -S83I, or -S83I/F89A and pBD constructs containing the same mutations. Figure 5 reveals that the F89A mutation, when present in both monomers, interferes with dimerization to a significant extent. S83I, on the other hand, markedly increases the extent of transcriptional activation, i.e., forms a dimer that is more stable than WT S100P. Moreover, introducing the S83I mutation compensates for the negative effect of the F89A substitution in the resulting double mutant. Thus, S83I is a gain-of-stability mutation, supporting the view that a hydrophobic side chain at the homologous position in other S100 proteins participates in mediating subunit contacts in the dimer.

As compared to the other dimer contacts described above, A-7 is a side chain with less hydrophobic character which is located at a position implicated in intermonomer contacts, e.g., through NMR analysis of holo-S100B (15). Due to this limited hydrophobic character, it was tempting to speculate that the introduction of a more hydrophobic side chain at position 7 would produce another gain-of-stability mutant dimer of S100P. To test this possibility, we generated an A7I mutant derivative and analyzed its capability to interact with itself, with WT S100P, or with the other S100P mutants

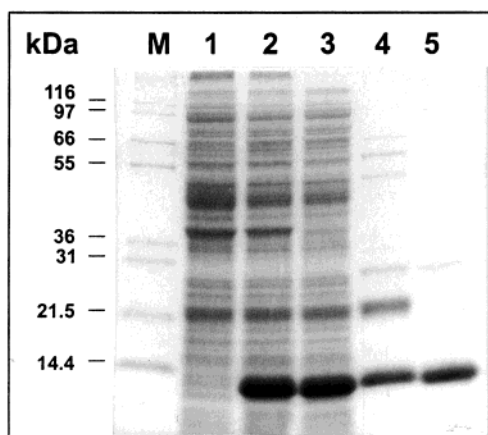


FIGURE 4: F15A S100P is stably expressed as a recombinant protein in *E. coli* cells. F15A S100P cDNA was cloned into pET28a+ (Novagen), and the resulting construct encoding F15A S100P with an N-terminal histidine tag was transformed into BL21(DE3)pLysS cells. The expression of recombinant protein was induced by adding IPTG to the culture. F15A S100P was then purified by chromatography on phenyl-Sepharose (Pharmacia) and subsequently on Ni-NTA agarose (Qiagen): lane M, molecular mass standards with the indicated sizes; lane 1, total cell lysate of an induced culture harboring the empty pET28a+ vector; lane 2, total cell lysate of an induced culture harboring the pET28a+-F15A S100P construct; lane 3, soluble fraction of the bacterial lysate (lane 2) after high-speed centrifugation; lane 4, protein eluted from phenyl-Sepharose with 30% 2-propanol; and lane 5, F15A S100P obtained following Ni-NTA agarose chromatography. Note that F15A S100P (apparent molecular mass of ~12 kDa) is expressed as a soluble protein and can be purified by two subsequent chromatographic steps.

by subjecting yeast cells transformed with the respective AD and BD constructs to growth on selective media and  $\beta$ -galactosidase activity assays. No interaction was observed with any of these constructs, indicating that the S100P dimer does not tolerate the large isoleucine side chain at position 7 (not shown).

## DISCUSSION

Various biochemical and structural analyses have shown that S100 proteins form obligatory dimers, and dimerization is thought to be crucial for S100 proteins functioning in  $\text{Ca}^{2+}$  stimulus-response coupling (6). Recent crystal structures have supported this view as both S100A10 (p11) and S100A11 (S100C) form dimers in complexes with target peptides derived from their cellular ligands annexin II and I, respectively. Each dimer binds two target peptides, and contacts to each peptide are provided from both S100 subunits (11, 12). Thus, dimerization not only will determine the physical status of S100 proteins but can also regulate their properties as mediators of cellular responses to  $\text{Ca}^{2+}$  transients. Several S100 dimers have been characterized structurally by NMR spectroscopy and X-ray crystallography in recent years (7, 9–15, 25). However, with the exception of the MRP 8/14 (S100A8–S100A9) heterodimer, dimer formation had not been analyzed *in vivo*. Here we provide such *in vivo* results by employing the yeast two-hybrid system. We show that S100P homodimers form within cells and that homodimer formation is specific, not tolerating other S100 subunits. Moreover, we identify residues which are crucially important for dimerization *in vivo*. These hydrophobic amino acids are in positions usually occupied by hydrophobic residues in other S100 proteins when their

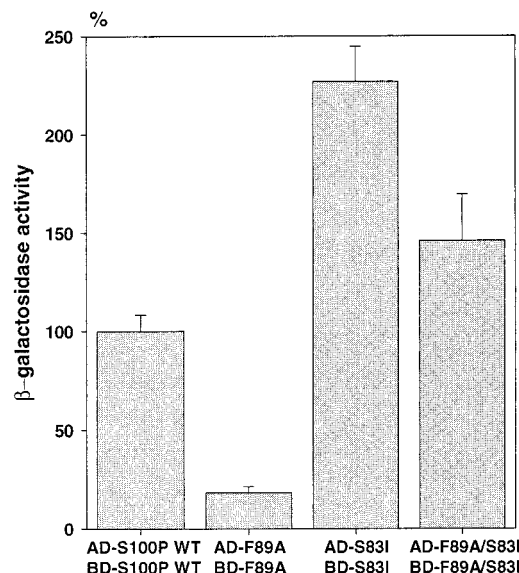


FIGURE 5: Quantification of  $\beta$ -galactosidase activity in cotransformed Y190 cells. Y190 cells were cotransformed with the indicated AD and BD plasmids and grown overnight in synthetic selection medium at 30 °C.  $\beta$ -Galactosidase activity was then determined in cell lysates as described in Experimental Procedures and taken as an indicator for the strength of the interaction between WT S100P chains or mutant S100P derivatives. AD- or BD-WT-S100P, activation domain or binding domain vector (pAD Gal4 amp or pBD Gal4 cam), respectively, containing the WT S100P insert. Here the resulting  $\beta$ -galactosidase activity was set to 100%. AD- or BD-F89A, activation domain or binding domain vector, respectively, with the S100P insert harboring the F89A mutation. AD- or BD-S83I, activation domain or binding domain vector, respectively, with the S100P insert harboring the S83I mutation. AD- or BD-F89A/S83I, activation domain or binding domain vector, respectively, with the S100P insert harboring the F89A and S83I mutations. Error bars indicate the standard deviation.

sequences are compared in a best-fit alignment. Previous structural analyses had revealed that such conserved hydrophobic side chains reside at the dimer interface most likely stabilizing the dimer through hydrophobic interactions. Most of the hydrophobic dimer contacts are found in helices I and IV of the individual S100 chains. By extrapolation of a general S100 fold to S100P, four of the mutations introduced here (I11A, I12A, F15A, and F89A) lie in these regions. F-15 proved to be essential for S100P dimerization as the F15A mutant protein, though expressed as a stable monomer, is not capable of forming complexes even with a WT S100P polypeptide. This indicates that the F-15 side chain is located at a crucial site of the dimer interface and that other hydrophobic contacts cannot compensate for a loss of hydrophobicity at this position even when present in only one subunit of the dimer. The scenario is somewhat different for I-11, I-12, and F-89. Here single-residue mutations, I11A, I12A, and F89A, hardly affect the interaction with WT S100P, whereas dimerization of two S100P subunits bearing such mutations is significantly compromised. Likewise, the level of interaction with WT S100P of the double mutant I12A/F89A is markedly decreased. As helices I and IV of the two S100P subunits in the dimer are most likely antiparallel [as seen in structural studies of other S100 proteins (7, 8, 11, 13–15, 25)], our findings suggest that I-12 of one subunit contacts F-89 of the other and that one such contact is dispensable for tight dimer formation. This is in line with previous biochemical analyses of S100A1 and



S100A11 which showed that elimination of the conserved hydrophobic residue located at a position homologous to F-89 in S100P does not affect dimerization (27, 29). Our in vivo data therefore underscore the importance of conserved hydrophobic dimer contacts previously noted in structural analyses of several S100 proteins (7, 8, 11, 13–15, 25) and also reveal that the individual side chains contribute differently to dimer stability.

One position occupied by a conserved hydrophobic residue implicated in dimer contact in other S100 proteins is occupied by a serine (S-83) in S100P. Interestingly, we could increase the level of interaction between S100P monomers when introducing an isoleucine instead of a serine at this position. Moreover, the strong inhibitory effect on dimerization of a F89A mutation introduced in the AD- and BD-S100P fusion proteins is offset when S-83 is replaced with I in one (or both) of the subunits. This represents the first gain-of-stability mutant for a S100 dimer and indicates that dimers can be modulated in vivo through the number of hydrophobic contacts. As dimers are the functionally relevant S100 species, it appears that S-83 in S100P has the function of destabilizing to some extent the S100P dimer. This could result in a more dynamic regulation of S100P function, e.g., in  $\text{Ca}^{2+}$ -regulated target protein binding. In an attempt to identify such targets, we screened a placental cDNA library using WT S100P as bait. However, even intensive screening ( $10^7$  clones) did not yield a candidate target protein. Most likely, this is due to the  $\text{Ca}^{2+}$  requirements for target protein binding which is not met in the environment of the yeast nucleus. Of all the S100 proteins, S100A10 is the only one exhibiting target (annexin II) binding in the absence of  $\text{Ca}^{2+}$ . It is therefore not surprising that the two-hybrid approach yields positive results for the S100A10–annexin II pair, whereas no signals are obtained for the biochemically well characterized but  $\text{Ca}^{2+}$ -regulated S100A11–annexin I pair (M. Koltzsch and V. Gerke, unpublished observations). Thus, methods differing from the standard two-hybrid approach have to be employed to identify targets of  $\text{Ca}^{2+}$ -regulated S100 proteins, including S100P.

## REFERENCES

1. Heizmann, C. W., and Cox, J. A. (1998) *Biometals* 11, 383–97.
2. Kretsinger, R. H. (1976) *Annu. Rev. Biochem.* 45, 239–66.
3. Kawasaki, H., and Kretsinger, R. H. (1995) *Protein Profile* 2, 297–490.
4. Zimmer, D. B., Cornwall, E. H., Landar, A., and Song, W. (1995) *Brain Res. Bull.* 37, 417–29.
5. Heizmann, C. W. (1999) *Neurochem. Res.* 24, 1097–100.
6. Donato, R. (1999) *Biochim. Biophys. Acta* 1450, 191–231.
7. Potts, B. C., Smith, J., Akke, M., Macke, T. J., Okazaki, K., Hidaka, H., Case, D. A., and Chazin, W. J. (1995) *Nat. Struct. Biol.* 2, 790–6.
8. Kilby, P. M., Van Eldik, L. J., and Roberts, G. C. (1996) *Structure* 4, 1041–52.
9. Potts, B. C., Carlstrom, G., Okazaki, K., Hidaka, H., and Chazin, W. J. (1996) *Protein Sci.* 5, 2162–74.
10. Drohat, A. C., Baldisseri, D. M., Rustandi, R. R., and Weber, D. J. (1998) *Biochemistry* 37, 2729–40.
11. Rety, S., Sopkova, J., Renouard, M., Osterloh, D., Gerke, V., Tabaries, S., Russo-Marie, F., and Lewit-Bentley, A. (1999) *Nat. Struct. Biol.* 6, 89–95.
12. Rety, S., Osterloh, D., Arie, J.-P., Tabaries, S., Seemann, J., Russo-Marie, F., Gerke, V., and Lewit-Bentley, A. (2000) *Structure* (in press).
13. Brodersen, D. E., Etzerodt, M., Madsen, P., Celis, J. E., Thogersen, H. C., Nyborg, J., and Kjeldgaard, M. (1998) *Structure* 6, 477–89.
14. Matsumura, H., Shiba, T., Inoue, T., Harada, S., and Kai, Y. (1998) *Structure* 6, 233–41.
15. Smith, S. P., and Shaw, G. S. (1998) *Structure* 6, 211–22.
16. Propper, C., Huang, X., Roth, J., Sorg, C., and Nacken, W. (1999) *J. Biol. Chem.* 274, 183–8.
17. Fields, S., and Song, O. (1989) *Nature* 340, 245–6.
18. Becker, T., Gerke, V., Kube, E., and Weber, K. (1992) *Eur. J. Biochem.* 207, 541–7.
19. Gribenko, A. V., and Makhatadze, G. I. (1998) *J. Mol. Biol.* 283, 679–94.
20. Laemmli, U. K. (1970) *Nature* 227, 680–5.
21. Schagger, H., and von Jagow, G. (1987) *Anal. Biochem.* 166, 368–79.
22. Isobe, T., and Okuyama, T. (1981) *Eur. J. Biochem.* 116, 79–86.
23. Teigelkamp, S., Bhardwaj, R. S., Roth, J., Meinardus-Hager, G., Karas, M., and Sorg, C. (1991) *J. Biol. Chem.* 266, 13462–7.
24. Wang, G., Rudland, P. S., White, M. R., and Barraclough, R. (2000) *J. Biol. Chem.* 275, 11141–6.
25. Drohat, A. C., Amburgey, J. C., Abildgaard, F., Starich, M. R., Baldisseri, D., and Weber, D. J. (1996) *Biochemistry* 35, 11577–88.
26. Kube, E., Becker, T., Weber, K., and Gerke, V. (1992) *J. Biol. Chem.* 267, 14175–82.
27. Seemann, J., Weber, K., and Gerke, V. (1996) *Biochem. J.* 319, 123–9.
28. Johnsson, N., and Weber, K. (1990) *J. Biol. Chem.* 265, 14464–8.
29. Osterloh, D., Ivanenkov, V. V., and Gerke, V. (1998) *Cell Calcium* 24, 137–51.

BI000257+